Enhanced thermal radiation in terahertz and far-infrared regime by hot phonon excitation in a field effect transistor

Pei-Kang Chung and Shun-Tung Yen

Articles you may be interested in

Voltage-controllable terahertz radiation from coherent longitudinal optical phonons in a p-i-n diode structure of GaAs
Appl. Phys. Lett. **103**, 141109 (2013); 10.1063/1.4823595

Degradation and phase noise of InAlN/AlN/GaN heterojunction field effect transistors: Implications for hot electron/phonon effects
Appl. Phys. Lett. **101**, 103502 (2012); 10.1063/1.4751037

Room temperature coherent and voltage tunable terahertz emission from nanometer-sized field effect transistors
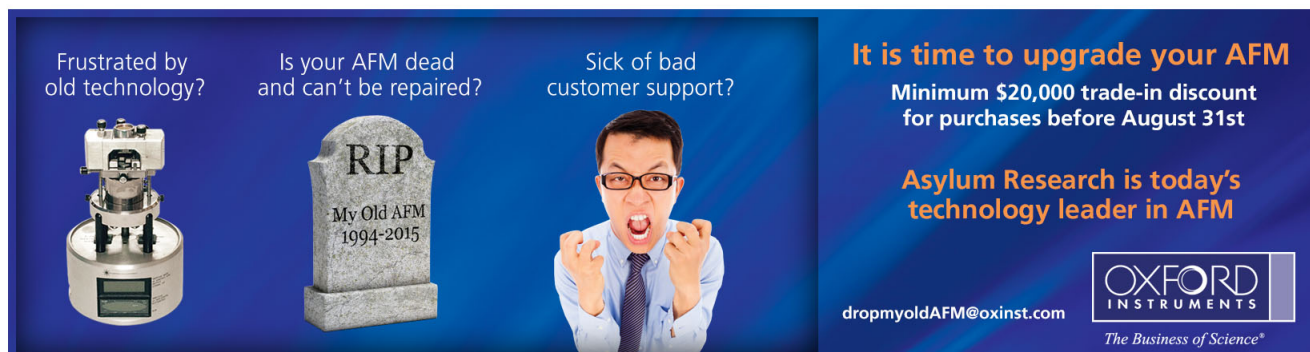Appl. Phys. Lett. **97**, 262108 (2010); 10.1063/1.3529464

Degradation in InAlN/GaN-based heterostructure field effect transistors: Role of hot phonons
Appl. Phys. Lett. **95**, 223504 (2009); 10.1063/1.3271183

Acoustic phonon scattering in a low density, high mobility Al Ga N ∕ Ga N field-effect transistor
Appl. Phys. Lett. **86**, 252108 (2005); 10.1063/1.1954893

Enhanced thermal radiation in terahertz and far-infrared regime by hot phonon excitation in a field effect transistor

Pei-Kang Chung and Shun-Tung Yen[a]
Department of Electronics Engineering and Institute of Electronics, National Chiao Tung University,
1001 Ta-Hsueh Road, Hsinchu, Taiwan

We demonstrate the hot phonon effect on thermal radiation in the terahertz and far-infrared regime. A pseudomorphic high electron mobility transistor is used for efficiently exciting hot phonons. Boosting the hot phonon population can enhance the efficiency of thermal radiation. The transistor can yield at least a radiation power of 13 μW and a power conversion efficiency higher than a resistor by more than 20%. © *2014 AIP Publishing LLC*. [http://dx.doi.org/10.1063/1.4901331]

I. INTRODUCTION

Terahertz and far-infrared radiation has been finding its wide applications in molecular or chemical detection,[1–3] non-destructive imaging,[1,2,4] high-speed communication,[5] and so on. There have been various types of radiation sources under intense study. Currently, practicable sources include thermal radiation lamps,[6] free-electron based radiators,[7] molecular gas lasers,[8] frequency mixers,[9] frequency difference generators,[10] solid-state current oscillators,[11] quantum cascade lasers,[12] and impurity-doped Ge or Si lasers,[13] etc. Solid-state thermal radiators have been considered a good candidate for wideband applications because they are compact, cheap, uncooled, and user-friendly such as simply electrically excited.[14,15] Conventional thermal radiators have a dielectric slab on which a metallic wire is deposited to heat the slab by electric current conduction.[15] Nevertheless, their applications generally focus on mid infrared and their power is weak in the terahertz/far-infrared regime.[15]

Conventionally, thermal radiation spectra are considered to depend only on the temperature and the surface emissivity of a radiator that is treated as a heat bath in thermal equilibrium.[16] Therefore, the radiation power is a function of temperature and hence the input power. In this paper, we report that the power and the efficiency of thermal radiation can be enhanced by selectively exciting hot phonons in a field effect transistor. The radiation spectrum depends not only on the input power but also on the means by which the electric power is imposed on the device. For a given electric input power, the transistor excited with a high voltage and a low current can yield a higher power conversion efficiency than a resistor excited with a low voltage and a high current. As a result, a single transistor can emit at least a thermal radiation of 13 μW in the spectral region between 2 and 20 THz and its power conversion efficiency can be higher than that of the resistor by more than 20%.

This paper is organized as follows. We describe the samples under study and the radiation measurement in Sec. II. We then present the results and discussion on the outputs of the devices in Sec. III. Finally, we draw a conclusion.

II. SAMPLES AND MEASUREMENT

The devices under study are an InGaAs channel pseudomorphic high electron mobility transistor (HEMT) and a GaAs resistor. The epitaxial layers of the HEMT [Fig. 1(a)], grown on a semi-insulating GaAs substrate, are a GaAs buffer layer, an InGaAs channel with a high-indium content sandwiched between two Si δ-doped ($\sim10^{12}$ cm^{-2}) AlGaAs barriers, and an n^+ GaAs cap layer. The cap layer serves as a medium to form ohmic contact with the source (S) and the drain (D) electrodes and is recessed for the gate (G) electrode, as the cross-section schematic in Fig. 1(b). As the layout [Fig. 1(c)] displays, the HEMT has a two-finger gate, an air-bridge source, and a drain. The distance between the source and the drain is $d = 2.5\,\mu$m. The gate length is $L = 0.15\,\mu$m. The channel width is $W = 100\,\mu$m. The sample containing the device is about $100\,\mu$m in thickness and 2×1 mm^2 in area. The resistor, used for comparison, has the same structure as the HEMT, except that the cap layer is not recessed and plays the dominant part in electrical conduction between the source and the drain. The samples are mounted on a printed circuit board (PCB) with thermal adhesive. The electrode pads are connected by gold wire bonding to metal contacts on the PCB for electrical biasing.

Radiation spectra and power were measured by a Fourier transform infrared (FTIR) spectrometer (Bruker IFS 66v/S). For quantitative measurement, careful calibration was performed on a Si bolometer, a deuterated-triglycine-sulfate (DTGS) detector, and the optical setup with a standard black-body radiator. The experiment was conducted with the samples uncooled and under the quasi-steady condition that the drain voltages V_D were applied with a duty cycle of 50% and a repetition rate of 12.5 Hz for later lock-in amplification of the detector output. The spectral resolution of the radiation was set at 10 cm^{-1}. Radiation from the fronts of the samples was collected for measurement.

III. RESULTS AND DISCUSSION

Figure 2 shows the electrical characteristics of the HEMT (with the gate voltages $V_G = -0.5$, 0, and 0.5 V) and the resistor. The HEMT behaves normally in the electrical characteristics except the slight decline in the current I_D with

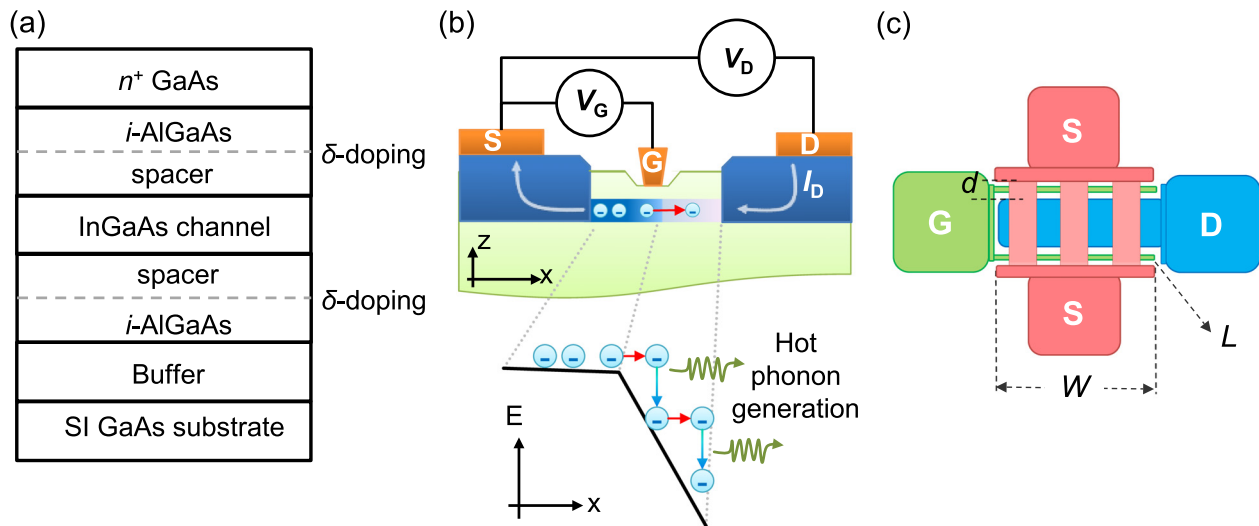[a]Electronic address: styen@nctu.edu.tw

FIG. 1. (a) Epitaxial layers of the investigated HEMT. (b) The cross section view of the HEMT biased in the saturation region and a schematic diagram showing hot phonon generation processes in the channel region. (c) The layout of the HEMT with a source-drain spacing $d = 2.5\,\mu$m, a gate length $L = 0.15\,\mu$m, and a channel width $W = 100\,\mu$m.

V_D in the saturation region due to the heating effect. Similarly, the resistor behaves sublinearly due to the heating effect as $V_D > 1$ V.

The inset of Fig. 2 shows radiation spectra of the HEMT, ranging up to 75 THz. Since we are currently interested only in the terahertz and far-infrared regime, we concentrate on the spectral region from 2 to 20 THz. Figure 3 shows the radiation spectra of (a) the HEMT (with $V_G = 0$ V) and (b) the resistor at various drain voltages V_D. The spectra exhibit several observable features at the spectral resolution of 10 cm^{-1}. The peaks at 13.3 and 15.6 THz are results of photon emission accompanied with phonon sum processes in GaAs [LO + LA(L) for 13.3 THz and IOΣ_1 + TOΣ_2 for 15.6 THz].[17] The apparent peaks at 7.4 and 9 THz result from the low radiation in the reststrahlen band about 8.2 THz.[18] The spectral positions of these features are basically unchanged

with V_D. The observation evidences that phonons in the GaAs substrate are responsible for the radiation. The phonons are excited via electron-phonon interactions in either the InGaAs channel of the pHEMT or the GaAs cap layer of the resistor.

The photon emission can be accomplished by phonon sum processes or phonon difference processes.[19] In polar crystals such as GaAs, a sum process involves virtually exciting a TO phonon at the Brillouin zone center by merging two phonons. The TO phonon is optically active and serves as the medium for emitting a photon.[19] Differently, in a difference process the TO phonon is virtually excited by absorbing a higher-energy phonon and emitting a lower-energy phonon.[19] The two-phonon processes are the dominant mechanism for thermal radiation in the terahertz and far-infrared regime.[19] Therefore, the relevant emission/absorption spectrum exhibits features which can correspond to features or van Hove singularities of the density-of-states spectrum of joint phonon branches.[20] Only the hot phonon modes, including the optical phonon modes and the acoustic phonon modes near the zone boundary, can contribute high density of states and hence result in dominant thermal radiation in the terahertz/far-infrared regime.[19]

As shown in Figs. 3(a) and 3(b), the spectral features grow remarkably as V_D (or the input power P_{in}) increases because of rising of the population of hot phonons that are involved in the sum processes. In light of the argument that the terahertz/far-infrared thermal radiation is enhanced by boosting hot phonon population, we create a critical issue: how to efficiently excite these phonons? The Fröhlich interaction is the most efficient for electrons to emit LO phonons in polar semiconductors if the electrons have sufficient kinetic energy.[21] With a given input power, a low flux of electrons driven by a high electric field is preferable for efficient generation of hot phonons to a high flux of electrons subjected to a low electric field. In the former case such as the case of the HEMT operated in the saturation region [Fig. 1(b)], electrons have a higher probability of gaining
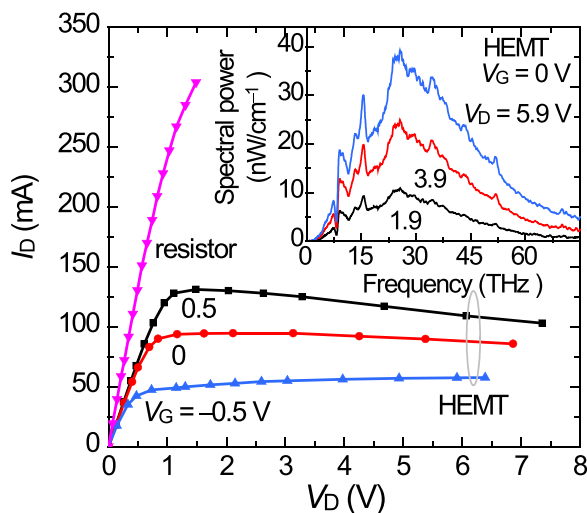

FIG. 2. The current–voltage characteristics (I_D versus V_D) of the HEMT (with $V_G = -0.5$, 0, and 0.5) and the resistor. The inset shows radiation spectra between 2 and 75 THz of the HEMT biased at $V_G = 0$ V and $V_D = 1.9$, 3.9, and 5.9 V.
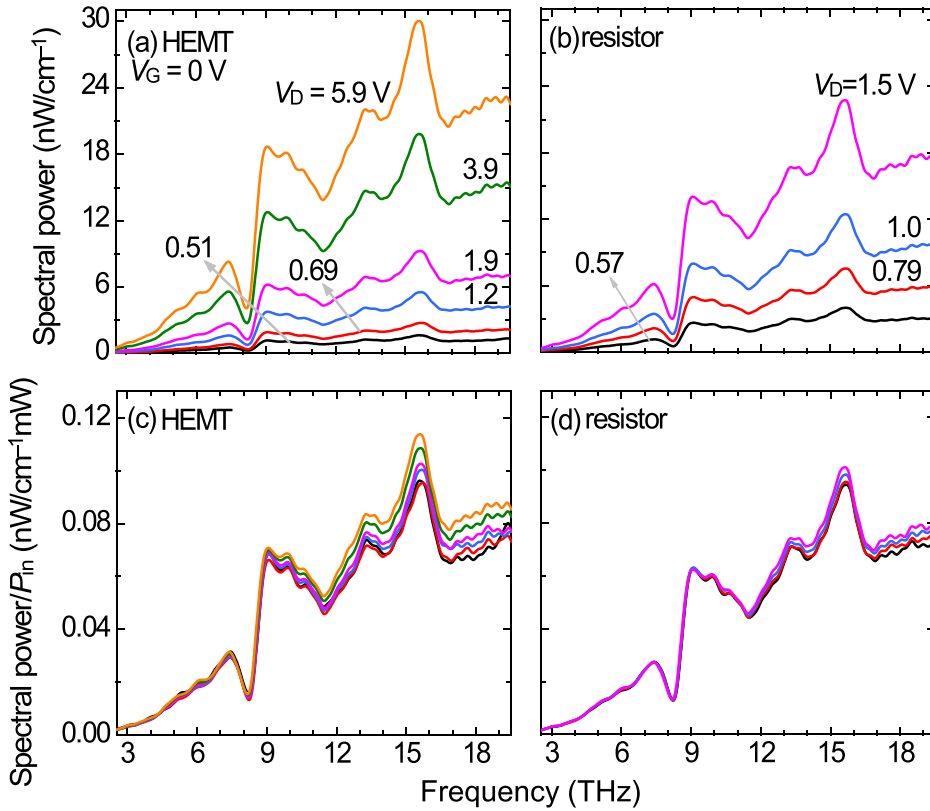
FIG. 3. Radiation spectra of (a) the HEMT biased at $V_G = 0$ V and $V_D = 0.51$, 0.69, 1.2, 1.9, 3.9, and 5.9 V and (b) the resistor at $V_D = 0.57$, 0.79, 1.0, and 1.5 V. Radiation spectra per unit input power for (c) the HEMT and (d) the resistor under the same bias conditions as in (a) and (b), respectively.

sufficient kinetic energy to emit hot phonons. The excited hot phonons then decay via the anharmonicity effect into other phonons either hot or cold, resulting in a nonequilibrium high population of hot phonons.[22] In the latter case, on the other side, such as the case of the resistor or the HEMT operated in the linear region, the hot phonon generation is not as efficient as for the former case, and the phonon population is likely to be quasi-equilibrium and describable with lattice temperature.

The HEMT has attractive advantages in hot phonon generation. It can control the electron flux by the gate voltage, easily build a high electric field in the channel between the gate and the drain by the drain voltage [Fig. 1(b)], and more importantly, provide an environment free from electron-impurity scattering.

The hot phonon effect not only enhances the terahertz/far-infrared thermal radiation but also boosts the radiation efficiency. This is evidenced by the data in Figs. 3(c) and 3(d), which show the radiation spectral power per unit input power for the HEMT (with $V_G = 0$ V) and the resistor, respectively, at various V_D. The spectral peaks at 13.3 and 15.5 THz grow with V_D more obviously than other spectral features because the peaks are related directly to the hot phonons. For the HEMT, the growth is even more remarkable as the device is driven into the saturation region. In contrast, the growth is milder for the resistor and also for the HEMT as operated within the linear region.

For practical applications, the radiation power level is important. Figure 4(a) shows the radiation power P_{out} versus the input power P_{in} for both the HEMT and the resistor. Here, the radiation power was measured with a calibrated DTGS detector combined with a low pass filter, which
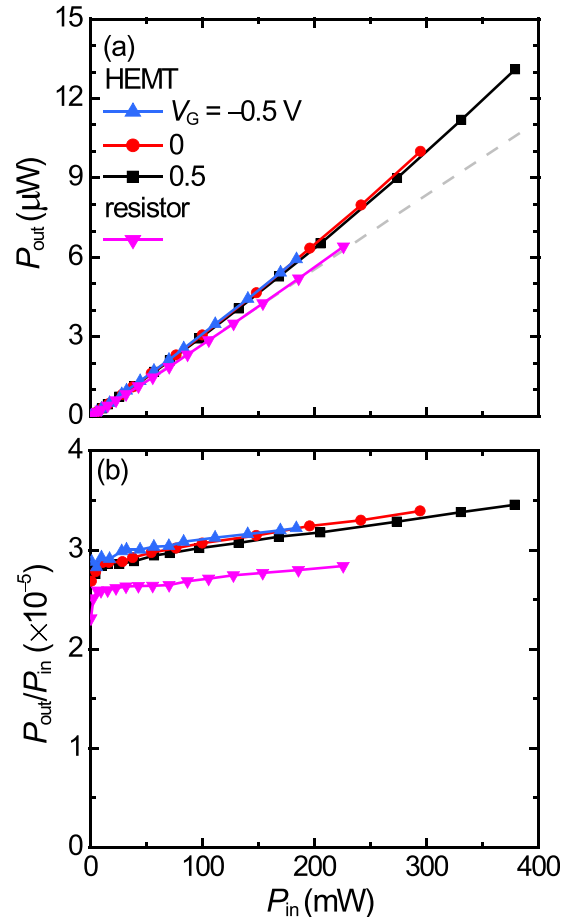

FIG. 4. (a) The radiation power P_{out} and (b) the power conversion efficiency P_{out}/P_{in} versus the input power P_{in} for the HEMT (biased at $V_G = -0.5$, 0, and 0.5 V) and the resistor.

detected the radiation below 20 THz. For $P_{in} > 6$ mW, the P_{out} varies almost linearly (in fact, slightly superlinearly) with P_{in} for the resistor, but in a more superlinear way for the HEMT due to the hot phonon effect. The curve for the resistor is under those for the HEMT, as expected according to the information in Fig. 3. The radiation power from a single device can reach a level as high as 13 μW.

Figure 4(b) shows the power conversion efficiency P_{out}/P_{in} versus the input power P_{in} for both the HEMT and the resistor. The HEMT has efficiencies always higher than the resistor at any given P_{in}. Furthermore, the three curves (with $V_G = -0.5, 0, 0.5$ V) for the HEMT in the saturation region are steeper in slope, and among them the one with a lower V_G has a steeper slope because it corresponds to a higher electric field in the channel at a given V_D. The efficiency of the HEMT can be higher than that of the resistor by more than 20% for $P_{in} > 200$ mW.

Apart from thermal excitation of hot phonons, hot plasmons can be effectively excited in the InGaAs channel and give rise to broadband terahertz emission (from 0.5 to 6.5 THz) at room temperature.[23] The spectral power due to hot plasmon excitation was estimated to be of the order of nW/cm^{-1}, on the same order as our devices emit. From our data, we cannot make conclusion on how important the hot plasmon excitation is to the radiation we observed. The clarification needs further study.

IV. CONCLUSION

We have investigated the hot phonon effect on thermal radiation in the terahertz and far-infrared regime. A high electron mobility transistor has been utilized for efficient hot phonon generation. The thermal radiation depends not only on the input power but also on the hot phonon population because the radiation is underlain by two-phonon processes involving hot phonons. Boosting the hot phonon population can increase the radiation power and also the power conversion efficiency. We have demonstrated that a single HEMT can emit a terahertz/far-infrared thermal radiation of 13 μW and have a conversion efficiency higher than a resistor by more than 20%. Our study provides a new way for engineering the thermal radiation spectrum by selective excitation of phonons.

[1]M. Tonouchi, Nat. Photonics **1**, 97 (2007).
[2]M. Walther, B. M. Fischer, A. Ortner, A. Bitzer, A. Thoman, and H. Helm, Anal. Bioanal. Chem. **397**, 1009 (2010).
[3]T. N. Brusentsova, R. E. Peale, D. Maukonen, G. E. Harlow, J. S. Boesenberg, and D. Ebel, Am. Mineral. **95**, 1515 (2010).
[4]W. L. Chan, J. Deibel, and D. M. Mittleman, Rep. Prog. Phys. **70**, 1325 (2007).
[5]T. Kleine-Ostmann and T. Nagatsuma, J. Infrared, Millimeter, Terahertz Waves **32**, 143 (2011).
[6]H. Rubens and R. W. Wood, Philos. Mag. **21**, 689 (1911).
[7]P. Tan, J. Huang, K. Liu, Y. Xiong, and M. Fan, Sci. China Inf. Sci. **55**, 1 (2012).
[8]E. Bründermann, H.-W. Hübers, and M. F. Kimmitt, Tetrahertz Techniques Springer Series in Optical Sciences Vol. 151 (Springer, Berlin, 2012), p. 109.
[9]J. C. Pearson, B. J. Drouin, A. Maestrini, I. Mehdi, J. Ward, R. H. Lin, S. Yu, J. J. Gill, B. Thomas, C. Lee, G. Chattopadhyay, E. Schlecht, F. W. Maiwald, P. F. Goldsmith, and P. Siegel, Rev. Sci. Instrum. **82**, 093105 (2011).
[10]Q. Y. Lu, N. Bandyopadhyay, S. Slivken, Y. Bai, and M. Razeghi, Appl. Phys. Lett. **104**, 221105 (2014).
[11]B. Razavi, IEEE J. Solid-State Circuits **46**, 894 (2011).
[12]B. S. Williams, Nat. Photonics **1**, 517 (2007).
[13]H.-W. Hübers, S. G. Pavlov, and V. N. Shastin, Semicond. Sci. Technol. **20**, S211 (2005).
[14]J. Hodgkinson and R. P. Tatam, Meas. Sci. Technol. **24**, 012004 (2013).
[15]J. Hildenbrand, J. Korvink, J. Wöllenstein, C. Peter, A. Kürzinger, F. Naumann, M. Ebert, and F. Lamprecht, IEEE Sens. J. **10**, 353 (2010).
[16]D. L. Stierwalt and R. F. Potter, *Optical Properties of III-V Compounds*, Semiconductors and Semimetals Vol. 3 (Academic Press, Inc., New York, 1972), p. 71.
[17]C. Patel, T. J. Parker, H. Jamshidi, and W. F. Sherman, Phys. Status Solidi B **122**, 461 (1984).
[18]M. Hass, *Optical Properties of III-V Compounds*, Semiconductors and Semimetals Vol. 3 (Academic Press, Inc., New York, 1972), p. 3.
[19]W. G. Spitzer, *Optical Properties of III-V Compounds*, Semiconductors and Semimetals Vol. 3 (Academic Press, Inc., New York, 1972), p. 17.
[20]E. S. Koteles and W. R. Datars, Can. J. Phys. **54**, 1676 (1976).
[21]P. Y. Yu and M. Cardona, *Fundamentals of Semiconductors-Physics and Materials Properties*, 4th ed. (Springer-Verlag, Berlin, 2010), p. 133.
[22]H. Hamzeh and F. Aniel, J. Appl. Phys. **109**, 063511 (2011).
[23]Y. M. Meziani, H. Handa, W. Knap, T. Otsuji, E. Sano, V. V. Popov, G. M. Tsymbalov, D. Coquillat, and F. Teppe, Appl. Phys. Lett. **92**, 201108 (2008).